



PERGAMON

Solid State Communications 119 (2001) 477–490

solid  
state  
communications

www.elsevier.com/locate/ssc

# High-pressure phases of the light alkali metals

N.E. Christensen<sup>a,\*</sup>, D.L. Novikov<sup>b</sup><sup>a</sup>*Institute of Physics and Astronomy, University of Aarhus, DK-8000 Aarhus C, Denmark*<sup>b</sup>*Arthur D. Little Inc., Acorn Park, Cambridge, MA 02140-2390, USA*

Received 13 June 2001; accepted 15 June 2001 by M. Cardona

## Abstract

Quantum-theoretical calculations are used to study high-pressure phases of sodium up to 500 GPa. Sixteen structures, mainly selected on the basis of experience obtained from experimental and theoretical high-pressure studies of other alkali metals, Li, Rb and Cs, are examined with respect to stability and pressure-induced structural transformations. Up to  $\approx 80$  GPa the bcc structure is favored, whereas Na-fcc exists between  $\approx 80$  and  $\approx 130$  GPa, where it becomes dynamically unstable and undergoes a rhombohedral distortion to  $hR1$ . At this pressure a multitude of lower coordinated structures have very similar enthalpies. The cubic  $cI16$  structure (as found for Li) may exist between 130 and 170 GPa. Among the structures examined, the calculations show that the Na phase with the lowest enthalpy has the  $CsIV$  structure between 170 and 220 GPa. Beyond 220 GPa a structure,  $oC8$ , with  $Cmca$  symmetry may be stable over a wide pressure regime. Whereas the  $s \rightarrow d$  transition determines the structural changes of Cs, the behavior of the light alkali metals under pressure is associated with an  $s \rightarrow p$  transition.

Although the emphasis is on sodium, new results for lithium are also presented, illustrating similarities and differences between the high-pressure behaviors of these two light alkali metals. At very high pressures Na may become an insulator, whereas so far we did not find any possible high-pressure Li-phases with a non-zero band gap. © 2001 Elsevier Science Ltd. All rights reserved.

PACS: 64.70.Kb; 71.15.Pd; 71.20.Dg

Keywords: A. Metals; C. Crystal structure and symmetry; D. Electronic band structure; D. Phase transitions

## 1. Introduction

The alkali metals, earlier considered as simple metals with band structures that differ only slightly from those of free-electron systems, have attracted considerable [1] interest because application of external pressure changes the bonding properties fundamentally. As a consequence, these metals undergo several pressure-induced structural transformations. These have been studied experimentally (see, for example, Refs. 2–8) as well as by theoretical methods (Refs. 7–20 and references therein).

For the heavy alkali metals, cesium and rubidium, the identification [4,21] of the structure of CsV and RbVI as being the orthorhombic  $Cmca$  structure with 16 atoms in the unit cell ( $oC16$ ) is important for the description of the pressure-induced changes in bonding and structure. The

same structure, with very nearly the same relative atomic coordinates, is found in Si and Ge under pressure [5,18,22–24]. This  $Cmca$  structure contains two types of atoms, say  $Cs_1$  and  $Cs_2$ , with  $Cs_1$  in planar arrangements separating  $Cs_2$  double layers. The atoms in the single planes form what appears as a dense packing of dimmers [18].

The light alkali metals, lithium and sodium, form at ambient conditions in the body-centered cubic structure, but their low-temperature phases have a more complex structure which was under debate for several years. It is now known [25–28] that both Li and Na undergo a martensitic transformation upon cooling to the  $9R$  structure (described in Section 2). In our calculations we cannot make reliable predictions about the zero-pressure structures (even) at  $T = 0$ . We did find [8] for Li that the  $9R$  structure is lowest in energy, but it is only  $\approx 1$  meV below Li-fcc, and for Na our calculations predict that either the body-centered cubic (bcc) or face-centered cubic (fcc) structure is stable at  $(P, T) = (0, 0)$ , but their energies are so close that

\* Corresponding author.

E-mail address: nec@ifau.au.dk (N.E. Christensen).

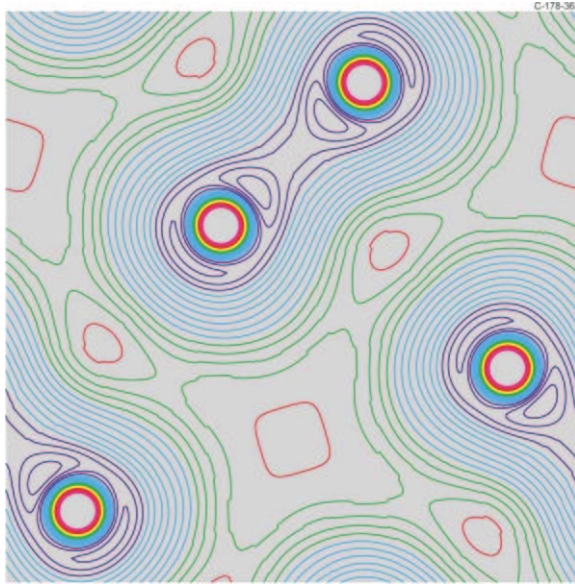


Fig. 1. Contour plot of the calculated valence-electron density in lithium in the *BC8* structure at 165 GPa ( $V/V_0 = 0.23$ ). The color coding is dark blue towards red/magenta for increasing density. The lowest contour value is  $0.0472 \text{ \AA}^{-3}$ , the increment is  $0.0135 \text{ \AA}^{-3}$ . Disregarding the innermost core oscillations, the highest valence density is found in the interstitial regime where the red (color changed from green for illustrative purpose) contour corresponds to the density  $\rho = 1.4 \times \rho_{av}$ , where  $\rho_{av} = 0.204 \text{ \AA}^{-3}$  is the average density. This picture is rather similar to what was found by Neaton and Ashcroft for *Li-oC8* in Ref. 11.

even structural difference in zero-point energy may affect the ordering. However, applying a small lattice expansion causes *Na-9R* to be energetically favored. Considering the high-pressure phases of Li and Na, Neaton and Ashcroft [11,17] first examined theoretically low-coordinated structures, including a *Cmca* structure showing a tendency to the formation of atomic pairs. This structure, so far not observed for the alkali metals, is also called *oC8*, and it has some similarity to *oC16* found for the heavy alkali metals, as mentioned above, but *oC8* only has half as many atoms in the primitive cell. The double layers of type-2 atoms are absent, i.e. the *oC8* structure is similar to that of Ga at ambient pressure. In Fig. 1 we show, as an example of such a 'paired structure', the distribution of valence electrons in lithium at 165 GPa. The apparent formation of atom pairs, however, should not be overemphasized. It is true that there is a single, shortest interatomic distance, but the next-nearest neighbors in the *Cmca* structures are not much farther away. Therefore the 'effective' coordination number in *Li-oC8* is rather  $\approx 5$  than one. The interesting result, though, is that there is a tendency of formation of low-coordinated phases of highly compressed alkali metals.

Experimentally, new high-pressure phases of lithium have been found, [8] *Li-hR1* and *Li-cI16*, and Hanfland

and Syassen [29]<sup>1</sup> have recently observed  $\text{bcc} \rightarrow \text{fcc} \rightarrow \text{cI16}$  transitions in Na. Sodium is then the second element for which the *cI16* structure, a 16-atom cubic supercell with displaced bcc atomic sites, has been observed.

The pressure-driven electronic  $s \rightarrow d$  transition [30] plays a major role in the structural behavior of cesium, [10,31] in particular for the occurrence of the tetragonal *CsIV* phase which is only eightfold coordinated [3]. The unusual decrease of the coordination number with increasing pressure from 12 in fcc to 8 in *CsIV* has been interpreted in terms of a peculiar multicenter bonding induced by the  $s-d$  transition [31,32]. The light alkali metals, Li and Na, are somewhat similarly influenced by an  $s \rightarrow p$  transition [33,34], as shown below.

The high-pressure phases of the alkali metals exhibit a variety of physical properties. At low pressures they are 'good' metals, but as will be shown, several high-pressure phases are characterized by having a very low [8,11,12,17] density of states at the Fermi level. In some cases the material may become a zero-gap semiconductor, and it appears that Na may even turn into an insulator. Another interesting feature is that lithium which is known not to superconduct at zero pressure, at least not above 4 mK, [35] may become a superconductor with a high value of  $T_c$  when pressure is applied [15,16].

Although the main emphasis is on sodium under pressure, we will also discuss new calculations for lithium. These will illustrate further the similarity between the behaviors of these two light alkali metals under pressure.

## 2. Structures

The ab initio simulation methods which we apply cannot be used to perform an ideal, molecular dynamical structural optimization. We must select a certain set of structure types, i.e. space groups (SG) and number of atoms in the cells. Some of the structures, however, will have parameters, like axial ratios and atomic site parameters, which must be optimized at each volume (pressure). We can then, among the structures included in the set, determine which one is stable (statically as well as dynamically) at a given volume. In that way one can never be sure to find the true ground state structure, but the procedure will be given relevance in predicting trends and bonding properties if the structures to be examined are selected in a 'sensible manner'. This section will present parts of the philosophy which we applied in our selection, and some of the less known structures will be described.

First of all, the set of structures should contain the usual close-packed structures, partly because they are known to occur at low pressures and partly because they may conform with the conventional point of view that coordination is

<sup>1</sup> M. Hanfland and K. Syassen have completed new experiments on Na up to 115 GPa.

expected to increase under pressure. But, on the other hand, we also know now that alkali metals and Group-IV semiconductors under very high pressures behave differently due to a change in binding caused by partial population of otherwise high-lying p and d states. Experimental as well as theoretical experience is then used to select a number of low coordinated structures as ‘good candidates’ for high-pressure Na phases. The most important experimental results which assist us in selecting ‘candidates’ are the recent observations [8] of the  $fcc \rightarrow hR1 \rightarrow cI16$  transition sequence in Li, and of the  $bcc \rightarrow fcc \rightarrow cI16$  transitions found [29] in Na. The simplest close-packed structures, bcc, fcc, and hexagonal close packed (hcp) are well-known. The hcp stacking sequence in the  $c$ -direction is ABA. Similarly, fcc and bcc can be built by stacking (111)-layers in the sequence ABCA. In this hexagonal representation, fcc has  $c/a = \sqrt{6}$ , and for bcc the axial ratio is  $c/a = 1/2 \times \sqrt{3/2}$ . The so-called  $\omega$ -phase [36] structure appears if the B and C layers in bcc are shifted so that they coalesce at  $z = c/2$ . The double-hexagonal close-packed structure (dhcp) has an ideal  $c/a$  ratio which is twice that of hcp, and the stacking is ABACA. The ‘samarium type structure’,  $9R$  is a nine-layer hexagonal structure, stacking ABABCBCACA. Calculations are most conveniently performed using the primitive rhombohedral cell which contains only three atoms. Also  $A7$  (arsenic structure, space group 166 in the International Crystallographic Tables) has a rhombohedral primitive cell. It contains two atoms. The basis vectors are:

$$\mathbf{a}_1 = a \left( \frac{1}{\sqrt{3}}, 0, \frac{c}{3a} \right); \quad \mathbf{a}_2 = a \left( -\frac{1}{2\sqrt{3}}, -\frac{1}{2}, -\frac{c}{3a} \right); \quad (1)$$

$$\mathbf{a}_3 = a \left( -\frac{1}{2\sqrt{3}}, \frac{1}{2}, \frac{c}{3a} \right),$$

and the atomic positions are:

$$\mathbf{r}_1 = (0, 0, uc); \quad \mathbf{r}_2 = (0, 0, -uc). \quad (2)$$

The special case where  $u = 1/4$  and  $c/a = \sqrt{3}$  yields the simple cubic, sc, structure. The simple rhombohedral structure,  $hR1$ , is obtained by removing the two atoms at the sites  $\mathbf{r}_1$  and  $\mathbf{r}_2$  and placing a single atom at  $\mathbf{r}_3 = (0, 0, 0)$ . It was observed in Li, [8] and is also included in the Na calculations here. The particular case where  $hR1$  has a  $c/a$ -ratio equal to  $\sqrt{6}$  corresponds to fcc, as mentioned earlier. In that case the rhombohedral angle,  $\alpha$ , is  $60^\circ$ . In the  $9R$  structure mentioned above all three sites are occupied. The structure which is called  $cI16$  belongs to the space group  $I\bar{4}3d$  (number 220 in the Int. Tab.). This was found experimentally for Li under pressure, [8] and until very recently [29] it had not been observed for any other elemental solid. The atoms are located in the 16c Wyckoff positions. The primitive cell is bcc, and an 8-atom basis is defined by the

coordinates (in units of  $a$ ):

$$(x, x, x); \quad \left( \frac{1}{4} + x, \frac{1}{4} + x, \frac{1}{4} + x \right);$$

$$\left( \frac{1}{2} + x, \frac{1}{2} - x, \bar{x} \right); \quad \left( \frac{3}{4} + x, \frac{1}{4} - x, \frac{3}{4} - x \right);$$

$$\left( \bar{x}, \frac{1}{2} + x, \frac{1}{2} - x \right); \quad \left( \frac{3}{4} - x, \frac{3}{4} + x, \frac{1}{4} - x \right);$$

$$\left( \frac{1}{2} - x, \bar{x}, \frac{1}{2} + x \right); \quad \left( \frac{1}{4} - x, \frac{3}{4} - x, \frac{3}{4} + x \right)$$

The structure reduces to bcc structure (‘supercell’ with eight usual cubic cells) for  $x = 0$ . The  $oC8$  structure of  $Cmca$  symmetry can be described by the primitive translations (using  $b$  as a unit):

$$\mathbf{a}_1 = \left( \frac{a}{2b}, -\frac{1}{2}, 0 \right); \quad \mathbf{a}_2 = \left( \frac{a}{2b}, +\frac{1}{2}, 0 \right); \quad (3)$$

$$\mathbf{a}_3 = \left( 0, 0, \frac{c}{b} \right),$$

and the atomic positions:

$$\mathbf{r}_1 = \left( 0, -y, z \frac{c}{b} \right); \quad \mathbf{r}_2 = \left( 0, y, -z \frac{c}{b} \right);$$

$$\mathbf{r}_3 = \left( 0, \frac{1}{2} - y, \left( z - \frac{1}{2} \right) \frac{c}{b} \right); \quad (4)$$

$$\mathbf{r}_4 = \left( 0, -\frac{1}{2} + y, -\left( z - \frac{1}{2} \right) \frac{c}{b} \right).$$

The theoretical study [11] of Li- $oC8$  is our motivation for including the  $oC8$  structure in our Li [8] and Na calculations [12]. For Na we find (Section 4) two different sets of structural  $oC8$  parameters. They are referred to as  $oC8$  and  $oC8-2$ . The former is close to the  $oC8$  structure found for Li, [8,11] whereas the latter is very close to the structure formed by the Si atoms in  $MoSi_2$ . It appears that some of the high-pressure phases have structures similar to the cation sublattices of binaries [8], and the structure of  $CsIV$  [3] is another example of this.  $CsIV$  forms in a tetragonal structure with  $I4_1/amd$  symmetry, SG 141, where the atoms are placed in

$$\mathbf{r}_1 = (0, 0, 0); \quad \mathbf{r}_2 = \left( 0, \frac{1}{2}, \frac{c}{2a} \right). \quad (5)$$

This is the structure of the Th sublattice in  $ThSi_2$  [37]. Therefore this was also included in the present study. The  $cI16$  structure described above is in fact that of the cation sublattice in  $Eu_4As_3$  and  $Yb_4As_3$ , i.e. anti- $Th_3P_4$  structures [38]. As already mentioned,  $cI16$  is a cubic structure with a bcc Bravais lattice and eight atoms in the primitive cell. Several other cubic structures may be generated by distorting such a bcc supercell. As one example we consider the  $BC8$  structure [39], mainly because it has been found, as also  $R8$ , in metastable Si and Ge phases [40–42]. The  $BC8$

structure is also body-centered-cubic with 16 atoms in the unit cell (eight atoms in the primitive cell). The space group is  $Ia\bar{3}$ , and the atoms are in the 16c Wyckoff sites,  $(x_0, x_0, x_0)$ . It may also be viewed as a rhombohedral structure with an 8-atom primitive cell, SG  $R\bar{3}$ . This has two atoms in the 2c,  $(u, u, u)$  and six in the 6f,  $(x, y, z)$ , sites. These parameters are related to  $x_0$  by  $u = 2x_0$ ,  $x = 1/2$ ,  $y = 0$ , and  $z = 1/2 - 2x_0$ . Thus, in  $BC8$  there is only one internal parameter ( $x_0$ ) which must be optimized.

The  $BC8$  structure can be considered as a special setting of the structural parameters of the  $R8$  structure. Both have the SG  $R\bar{3}$  (number 148). The eight atoms in the  $R8$  primitive cell are located at the 2c,  $(u, u, u)$ , and the 6f,  $(x, y, z)$ , Wyckoff sites. In  $BC8$  all the eight sites are equivalent, but in  $R8$  the 2c and the 6f sites are inequivalent. For  $R8$  we use the primitive translations as given in Eq. (1), and the atomic sites are:

$$\begin{aligned} \mathbf{r}_1 &= \left( x - (y+z)\frac{1}{2}, (y-z)\frac{\sqrt{3}}{2}, (x+y+z)\frac{c}{a} \right); \\ \mathbf{r}_2 &= \left( z - (x+y)\frac{1}{2}, (x-y)\frac{\sqrt{3}}{2}, (x+y+z)\frac{c}{a} \right); \\ \mathbf{r}_3 &= \left( y - (z+x)\frac{1}{2}, (z-x)\frac{\sqrt{3}}{2}, (x+y+z)\frac{c}{a} \right); \\ \mathbf{r}_4 &= \left( -x + (y+z)\frac{1}{2}, -(y-z)\frac{\sqrt{3}}{2}, -(x+y+z)\frac{c}{a} \right); \\ \mathbf{r}_5 &= \left( -z + (x+y)\frac{1}{2}, -(x-y)\frac{\sqrt{3}}{2}, -(x+y+z)\frac{c}{a} \right); \\ \mathbf{r}_6 &= \left( -y + (z+x)\frac{1}{2}, -(z-x)\frac{\sqrt{3}}{2}, -(x+y+z)\frac{c}{a} \right); \\ \mathbf{r}_7 &= \left( 0, 0, 3u\frac{c}{a} \right); \quad \mathbf{r}_8 = \left( 0, 0, -3u\frac{c}{a} \right). \end{aligned}$$

For  $c/a = \sqrt{2}/4$ ,  $y = 0$ , this specializes to  $BC8$ . If further  $u = 1/4$  ( $x_0 = 1/8$ ),  $BC8$  becomes identical to the bcc superstructure with SG 230 ( $Ia\bar{3}d$ ) and atoms in the equivalent 16b positions. The  $BC8$  and  $R8$  were predicted to be among the possible candidates for structures of Li phases at very high pressures [8,12].

Our calculations [12] have shown that the graphite form of lithium has a lower enthalpy than  $oC8$ -Li when the pressure exceeds 300 GPa. The graphite structure consists of hexagonal layers in an ...ABAB... sequence so that half the atoms in a layer are directly above and below the atoms in the adjoining layers, and the other half are directly above and below the centers of the hexagons. The space group is  $P6_3/mmc$  (Nr. 194) with atoms in the 2b and the 2c positions, Pearson symbol  $hP4$ . At a given volume, only one parameter,  $c/a$ , has to be optimized. In addition to this,

we also included another structure where the stacking of the layers with hexagons is ...AAAA....

### 3. Methodology

The total energy of the electrons for a given choice of atomic coordinates (structure and volume) is calculated within approximations to the density functional theory, the local approximation (LDA) as well as a generalized gradient approach (GGA). The results presented here are obtained with the GGA, and we used the Perdew–Burke–Ernzerhof scheme [43]. The solution of the effective one-electron equations is performed by means of the linear muffin-tin-orbital (LMTO) method [44] in the full-potential version [45]. The band structure calculations are scalar relativistic, i.e. all relativistic effects, except spin–orbit splittings, are included. Concerning the choice of basis set, the present sodium calculations are similar to those used earlier [7,8,18–20] for the high-pressure phases of Cs, Li, and Na. This means that a ‘triple- $\kappa$  basis’ [45] is used, and in each channel we include s-, p-, d-, and f partial waves. Semi-core states, 1s in lithium, 2s and 2p in sodium, are treated as local orbitals [46] (LO) and included among the usual valence states. The Na-1s states are treated as atomic-like states relaxed in the crystal potential. The structural optimization required in all cases except for the bcc and fcc structures is made at each of 21 volumes,  $V$ , in the range  $0.10 \times V_0$ – $1.10 \times V_0$ , where  $V_0$  is the (experimental) equilibrium volume of bcc-Na at ambient pressure, corresponding to the lattice constant  $a = 4.225 \text{ \AA}$ . (We use  $V_0 = 21.2725 \text{ \AA}^3$  for Li and  $37.7073 \text{ \AA}^3$  for Na). For some structures, like hcp, dhcp, and  $hR1$ , only a single, internal parameter needs to be varied, but other cases require more time consuming optimizations.  $A7$  and  $9R$  require optimization of two parameters,  $z$  and  $c/a$ . In the  $Cmca$  structures we need to vary the axial ratios,  $c/a$  and  $b/a$ , as well as two (in  $oC8$ ) or three (in  $oC16$ ) internal parameters. Also for  $R8$  there are five parameters to be optimized simultaneously. This is done by means of a steepest-descent method.

### 4. Results

Having calculated the optimized total energies,  $E$ , vs. volume for all structures, and applying a least-squares fit to a power series in  $X = (V/V_0)^{1/3}$  (positive as well as negative powers), we derive pressure,  $P$ , bulk modulus,  $B$ , and enthalpy,  $H = E + PV$ . The calculated  $P$ – $V$  relations are then used to calculate  $H(P)$ , and the results for Na are summarized in Fig. 2. The enthalpies of  $oC16$  have been omitted, since for Na (as for Li) its energy is far above those of the other structures. At low pressures (not visible on the scale of Fig. 2) we find that the bcc structure is favored in sodium. The calculation predicts that this remains the stable structure up to  $P_{t1} \approx 80 \text{ GPa}$ , where it transforms to fcc. It should be noted, however, that the maximum difference,

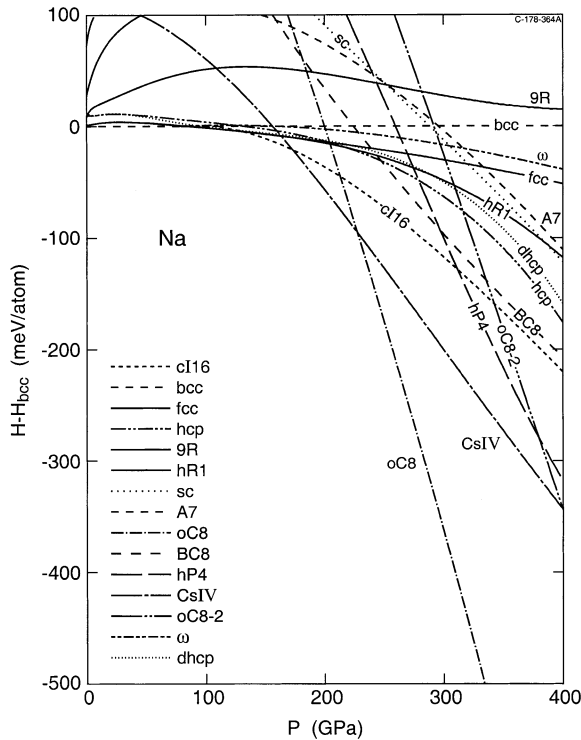


Fig. 2. Enthalpies of 15 Na phases vs. pressure ( $P$ ). The enthalpy of the bcc structure is used as a reference.

$E(\text{fcc}) - E(\text{bcc})$  is only 5 meV/atom. (Same differences were obtained by using the straight LDA). The fact that we find the energy difference to be that small also implies that a substantial error bar is associated with the value of  $P_{11}$ . The instability of Na-bcc is also reflected in the volume dependence of the elastic shear constants. As found by Katsnelson et al. [9] and also in the calculations [19,20] for Cs,  $C'$  and  $C_{44}$  soften and tend to go negative under compression. This may also be illustrated by the energy dependence on axial ratio,  $c/a$ , in Na-bct as shown in Fig. 3. At large volumes,  $V/V_0$  above  $\approx 0.30$ , the energy minimum is at  $c/a = 1.0$  (bcc), but a secondary minimum appears near 1.4. For smaller volumes this becomes the low-energy structure with  $c/a = \sqrt{2}$ (fcc). Another distortion of the bcc structure of sodium could be possible, namely that to the  $\omega$ -phase. Fig. 4 shows the energy variation calculated as functions of  $\delta$ , the displacements of the B- and C layers towards the central position in bcc as a hexagonal stacking. The value  $\delta = 1/6$  corresponds the  $\omega$ -phase where B and C have coalesced. For  $V/V_0 \approx 0.22$  we find (Fig. 4) that only tiny energy changes are involved when the B and C layers are moved. If Na had preferred to distort to the  $\omega$  phase in the corresponding pressure regime, a dramatic softening of the  $\Lambda(2/3, 2/3, 2/3)$  LA phonon in Na-bcc would have taken place. At high pressures, Fig. 2 clearly shows that Na- $\omega$  cannot be a stable structure.

The (perfect) fcc (Fig. 2) structure remains stable up to

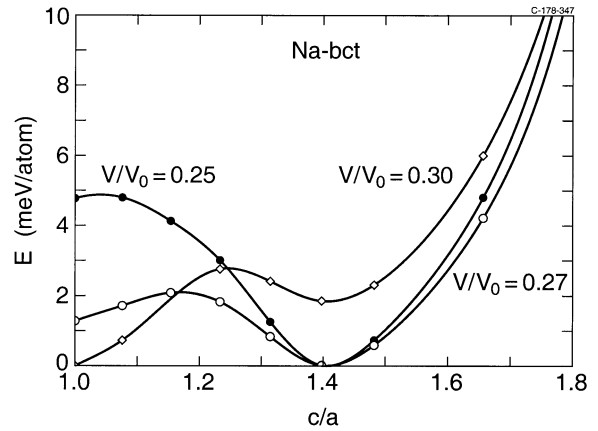


Fig. 3. Energy of Na-bct vs.  $c/a$ -ratio at the bcc  $\rightarrow$  fcc transition for three volumes. (The axial ratio  $c/a = 1$  corresponds to bcc, whereas  $c/a = \sqrt{2}$  represents the fcc structure).

$\approx 130$  GPa, where it becomes unstable against a rhombohedral shear. The elastic constant  $C_{44}$  goes negative, and the fcc-lattice becomes dynamically unstable. This signals the transition to the distorted structure,  $hR1$ . In lithium the  $hR1$  phase has a structure which appears as a compression [8] along the fcc body diagonal (see Fig. 5). Sodium behaves differently in the sense that in Na- $hR1$   $c/a$  is larger than  $\sqrt{6}$ , the fcc value (see Figs. 6(a) and (b)). Experimentally, however, this will probably not be observed since the  $cI16$  structure is energetically favored even over Na- $hR1$  in the same pressure range. The calculated onset of Na- $cI16$  is around  $P_{12} \approx 130$  GPa, somewhat higher than observed [29] 100 GPa. It is interesting to note, on the other hand, that the calculation by Neaton and Ashcroft [17] also predicts the transition pressure to be 130 GPa, although a

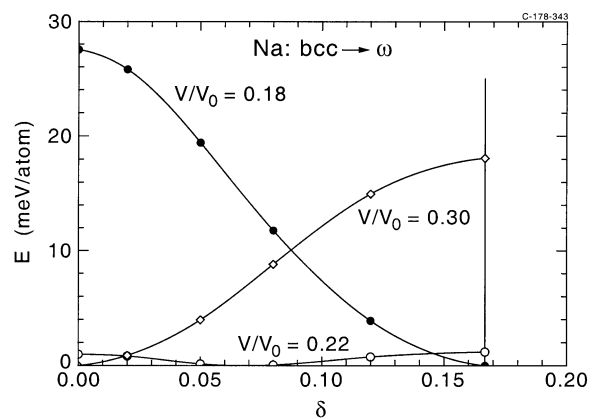


Fig. 4. Energy of Na-bcc distorted towards the  $\omega$  structure for three volumes. The parameter  $\delta$  gives shifts (up/down along the  $c$  axis in the hexagonal representation) of the B and C layers. The layers coalesce for  $\delta = 1/6$ . The results for  $V/V_0 = 0.22$  illustrate that the bonds at that volume become extremely soft.

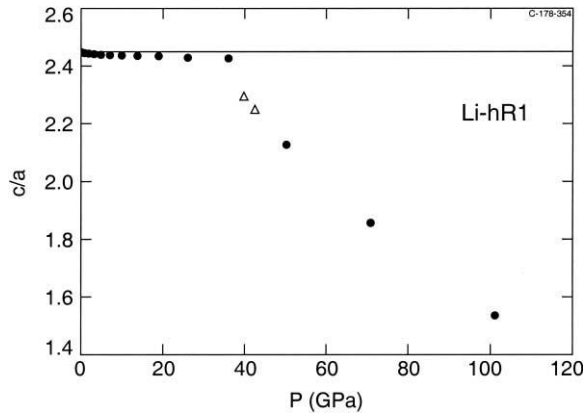


Fig. 5. Axial ratio,  $c/a$ , of *Li-hR1* versus pressure. The two triangles represent the experiments of Ref. 8. The filled circles are obtained by the theoretical optimization and pressure calculations.

different band structure calculation method was used. (Our earlier calculation [12] yielded a somewhat higher value of the pressure at which Na should transform to *cI16* due to a too low packing fraction with muffin-tin spheres in the distorted structure.) The displacements,  $x$ , increase with

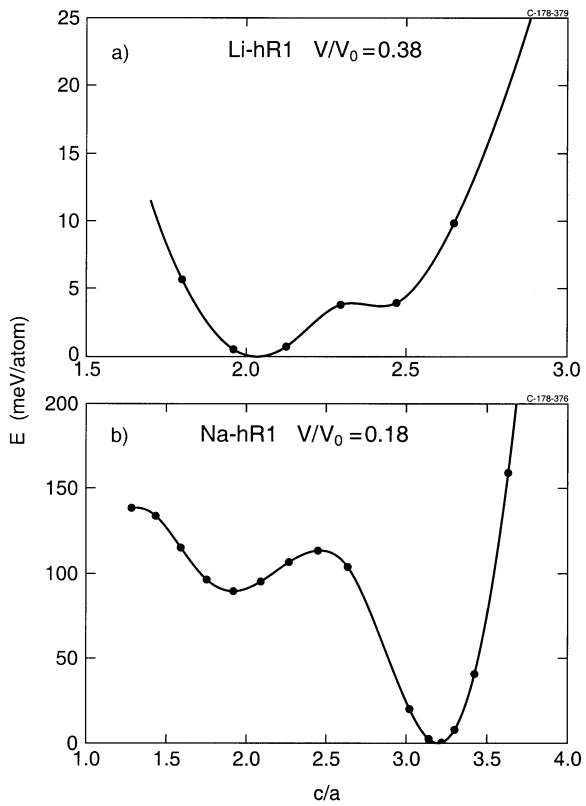


Fig. 6. Variation of the total energy of (a): *Li-hR1* and (b): *Na-hR1* vs. axial ratio,  $c/a$ . The volumes are fixed to  $V = 0.38 \times V_0$  (Li) and  $V = 0.18 \times V_0$  (Na). The fcc structure corresponds to  $c/a = \sqrt{6}$ .

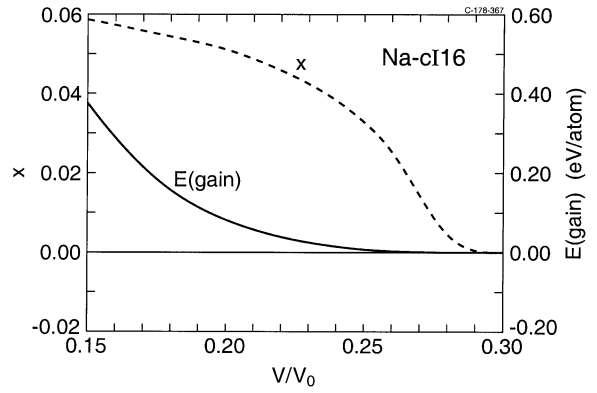


Fig. 7. Displacement  $x$  in *Na-cI16* and the energy gained by the relaxation to finite  $x$  vs. volume. The structure is bcc ( $x = 0$ ) for all  $V/V_0$  larger than  $\approx 0.29$ .

compression (see Fig. 7) and seem to approach a limiting value of 0.065 at extreme compressions. This is different from Li, where a saturation value of 0.125 was found [8]. The energy gained,  $E(\text{gain})$ , by relaxation to a finite  $x$ -value increases with compression as shown in Fig. 7. The *cI16* structure is energetically favored up to  $P_{13} \approx 170$  GPa, a pressure regime where *Na-CsIV* rapidly lowers its free energy with pressure so that it becomes the one with lowest

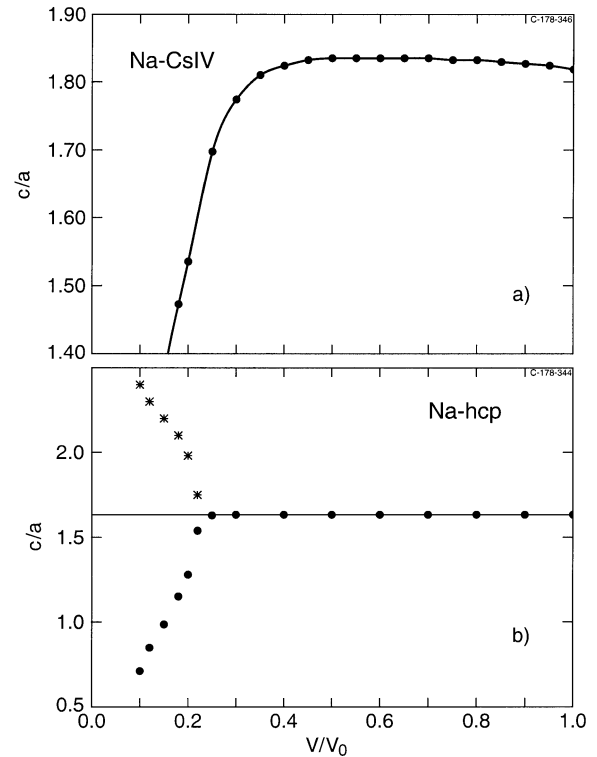


Fig. 8. Axial ratio for Na in (a): the *CsIV* structure and (b): the hcp structure as functions of volume.

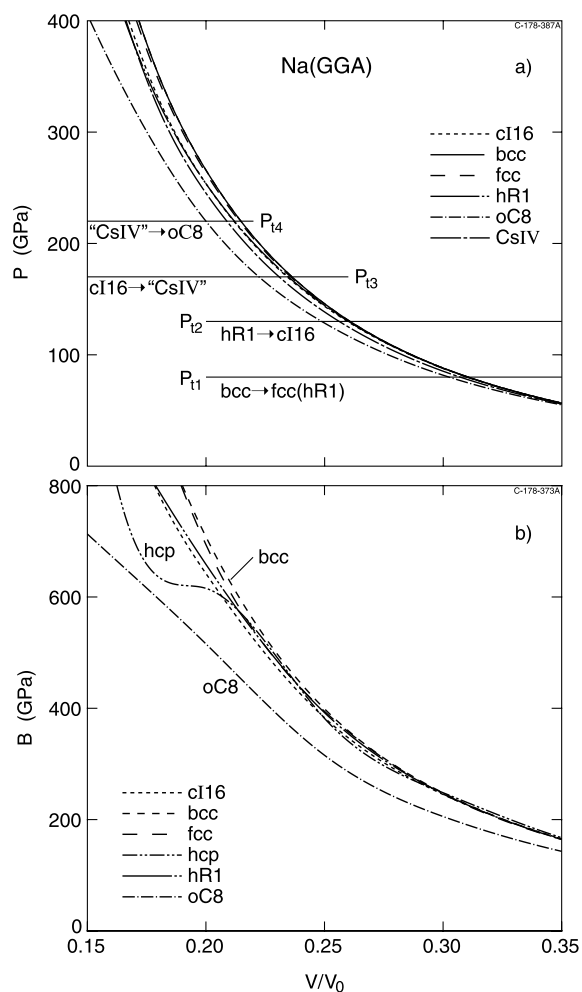


Fig. 9. Pressures (a) and bulk moduli (b) vs. volume for Na in selected structures between 0.15 and 0.35  $V_0$ .  $P_{11}$ ,  $P_{12}$ ,  $P_{13}$ , and  $P_{14}$  are the calculated pressures of transition from bcc to fcc/hR1, hR1 to cI16, cI16 to 'CsIV', and 'CsIV' to Na-oC8.

energy among the structures examined up to  $P_{14} \approx 220$  GPa, where the  $Cmca$  structure, oC8, takes over. One should bear in mind, however, that the energy error bars are  $\approx 5$  meV/atom, at best. In lithium a larger stability range was predicted [8], but also in that case the CsIV structure may push the upper limit down (see later). For Na-CsIV the  $cla$  ratio had to be optimized, and the calculated volume variation is shown in part (a) of Fig. 8.

Apart from the range from 120 to 200 GPa where several structures are close in energy, the hexagonal hcp structure is not likely to be a 'good candidate' for Na at high pressure, although substantial energy can be gained by reducing  $cla$  at small volumes (Fig. 8(b)). At the volume  $V = 0.25 \times V_0$ , as well as for all volumes larger than this, we find a single energy minimum at the ideal  $cla$  ( $\sqrt{8/3}$ ), but the ideal hcp structure becomes unstable upon compression. Actually,

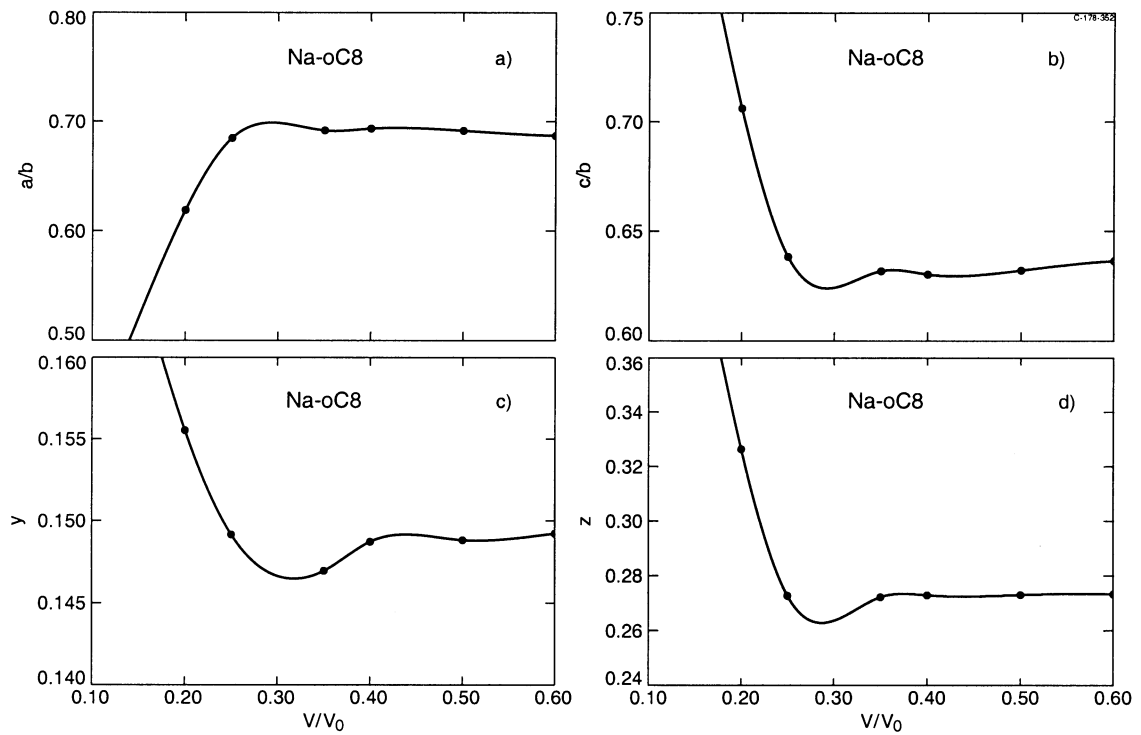
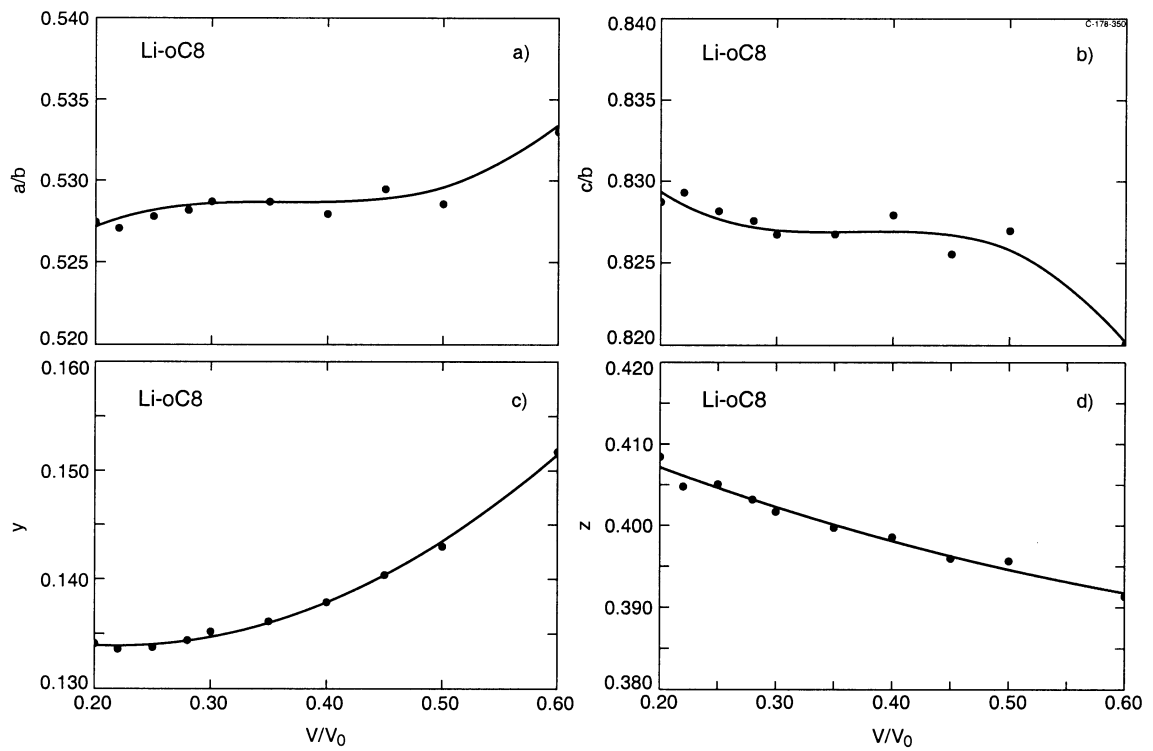
two new minima develop, one at a smaller axial ratio, and one at a larger value. The latter minimum is always higher, i.e. it corresponds to a metastable structure. Fig. 8(b) shows how the  $cla$ -values corresponding to the global minimum (dots) and the higher-lying minimum (asterisks) vary with volume. Similar results were obtained in Ref. 9. The dhcp structure exhibits a different behavior. It becomes unstable for volumes around  $V/V_0 = 0.22$ , and the enthalpy curve plotted for Na-dhcp has no physical meaning above  $P \approx 220$  GPa. It remains to be examined whether a dhcp (or related) structure again can stabilize when  $P$  is increased further, similarly to what was calculated for the  $\omega$  phase. The four coexistence pressures  $P_{11}$ ,  $P_{12}$ ,  $P_{13}$  and  $P_{14}$  are also marked in Fig. 9(a) which shows the calculated  $P$ - $V$  relations for some selected structures of Na at small volumes. From low pressures (in fact from 0) up to 120 GPa we find that the pressures of the close-packed phases follow each other closely. A change of slope in  $P(V)$  for hcp-Na around 270 GPa reflecting the rapid change in  $cla$  upon compression is illustrated in Fig. 8(b). This becomes even more pronounced in the variation of the bulk modulus (Fig. 9(b)). Similar effects of the structural relaxations appear in hR1 and oC8, although less dramatic than for hcp.

At very high pressures Na-oC8 clearly has the lowest free energy in Fig. 2. The variation of the structural parameters (as defined in Section 1) with volume is shown in Fig. 10. These results are somewhat different from those found for lithium (see Fig. 11). For Na we also found higher-lying local minima in the oC8 energy surface, and these solutions correspond to the enthalpy curve labeled oC8-2 in Fig. 2. The structural parameters of oC8-2 are rather different. Within very small margins,  $a$  and  $c$  are equal to  $0.5883 \times b$  over the entire volume range considered, and  $z$  stays fixed at 0.5. Only  $y$  varies.

#### 4.1. Electronic structure and phase stability

This section describes the electronic structures of sodium in selected crystal structures. The relation between the energy distributions of the valence electrons and the structural stability is examined, and also the  $s \rightarrow p$  transition is illustrated.

First, Fig. 12 shows the density of states (DOS) functions in the valence-band regime for Na-bcc, -fcc, and -hR1. Also, partial 3s- and 3p-DOS functions are shown for the bcc phase. The volume chosen here is  $V/V_0 = 0.25$ , i.e. the pressure is above  $P_{11}$ , the calculated bcc/fcc coexistence pressure for Na. The total bcc-DOS exhibits a smooth, featureless free-electron like behavior for all energies below the Fermi level,  $E_F$ . The same is the case for the fcc-DOS at this volume, and in fact it cannot be easily distinguished from the bcc-DOS in this energy regime. The bcc-fcc energy difference is indeed very small, and the fact that Na-fcc is lower in energy than Na-bcc at this volume cannot be clearly ascribed to differences in the one-particle

Fig. 10. Volume variation of the structural parameters of the *oC8* structure of Na.Fig. 11. Volume variation of the structural parameters of the *Li-oC8*.

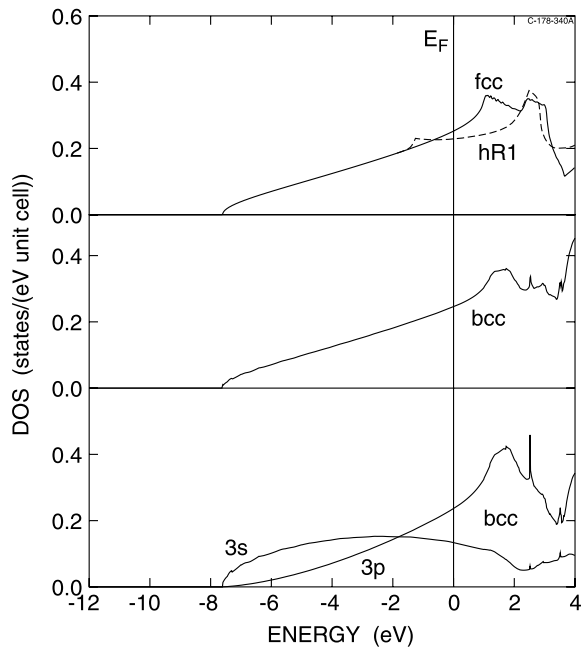


Fig. 12. Density-of-states functions for Na in the bcc, fcc, and *hR1* structures at  $V/V_0 = 0.25$ . The *hR1* DOS is identical to that of Na-fcc, except for the part shown as a dashed curve. Lowest panel: occupied parts of valence s- and p contributions to the bcc DOS. The d- and f- contributions are not shown.

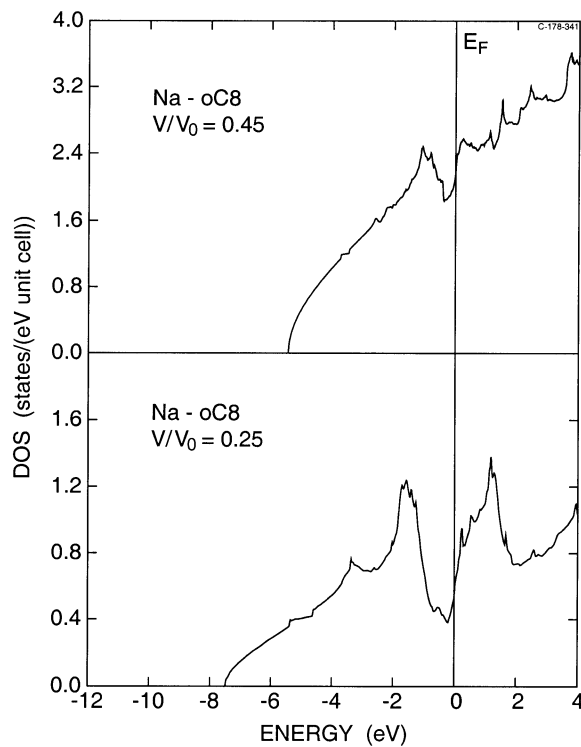


Fig. 13. Density-of-states functions of Na in the *oC8* structure at  $V/V_0 = 0.45$  (upper part) and  $0.25$  (lower part).

energy distribution. Details in the Coulomb interactions (including exchange-correlation) must play a major role in this connection. Fig. 12 (upper part), on the other hand, shows that the transition from Na-fcc to *hR1* (the rhombohedrally strained fcc) is associated with a decrease in band-structure energy. The saddle point in the p-DOS which in Na-fcc lies above  $E_F$  has in *hR1* moved below the Fermi level, and consequently occupied electronic states have been moved to lower energies. The one-electron energy distribution thus favors the *hR1* structure over fcc.

For Li it was demonstrated [8] that the distortion (finite  $x$  value in Fig. 7) of the bcc structure into *cI16* is accompanied by the formation of a pseudo-gap, and thus to a downshift in energy of an appreciable amount of filled electron states. The one-electron energy sum is similarly reduced in Na-*cI16* as  $x$  becomes non-zero. A similar effect is found in the *CsIV* structure, and in Na-*BC8* we find that a pseudo-gap near  $E_F$  tends to stabilize the structure. In all cases the increasing occupation of p states with pressure is essential for the formation of the new structures, and this is most spectacular in Na-*oC8*, the phase which is clearly the lowest in energy among those examined in the high-end of the pressure range of Fig. 2. The pseudogap which is present even at  $V/V_0 = 0.45$  (Fig. 13) becomes rapidly deeper as the lattice is compressed (lower part of Fig. 13) and near  $V/V_0 = 0.12$ , the DOS at  $E_F$  vanishes. Upon further compression a non-zero gap opens in the band structure of Na-*oC8*; Fig. 14 shows its position in the Brillouin zone for  $V/V_0 = 0.10$ . In Li-*oC8* it was also found [8,11] that  $DOS(E_F)$  vanishes at a very high pressure, but the energy-optimized structure did not exhibit a non-zero gap. Neaton and Ashcroft noted [11] that a small change in the structure (Peierls distortion) could produce a gap in the band structure of lithium, but the associated gain in one-particle energy

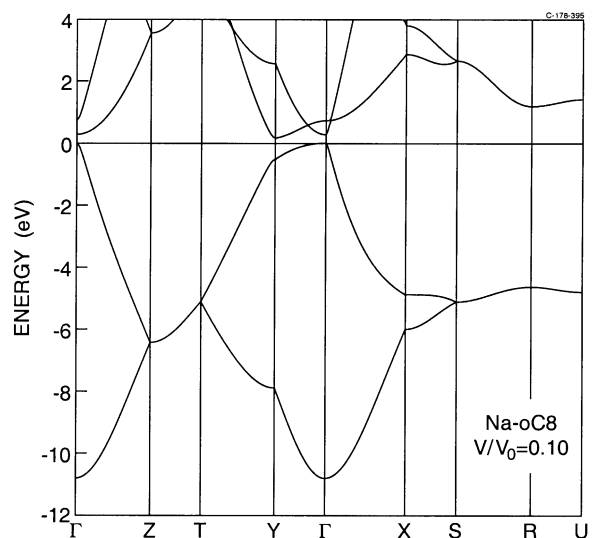


Fig. 14. Band structure of the *oC8* structure at  $V/V_0 = 0.10$ . The horizontal line (zero energy) marks the valence-band maximum.

(band structure energy) was not sufficient to compensate for the increase in Coulomb (exchange-correlation) energy, and the distorted phase would not be stable.

The  $s \rightarrow p$  transition responsible for this behavior is further illustrated in Fig. 15(a). The very strong increase in the ratio between p- and s electron counts at large compressions is very much like what is found for lithium (see Fig. 15(b)). At first, such a behavior might be explained for Li as an effect of orthogonality; the Li atom has a full 1s core, and the 2s valence states are kept away from the core region, even at small volumes due to their orthogonality to the 1s states. Orthogonality does not impose a similar radial constraint on the Li-2p states, and consequently the 2p canonical band [44] can increase its overlap with the Li-2s band when Li is compressed. This is illustrated for Li-fcc in Fig. 16. But a similar argument cannot be applied strictly to Na. In that case the core of the atom contains s- as well as p-states (2p), and a weaker  $s \rightarrow p$  transition should then be expected. The simplified picture, however, is based on a crude model without hybridization and hybridization is very strong in the compressed alkali metals. If we consider a hypothetical Na-fcc crystal at the smallest volume ( $V = 0.1 V_0$ ) considered here, its interatomic distance is 1.73 Å.

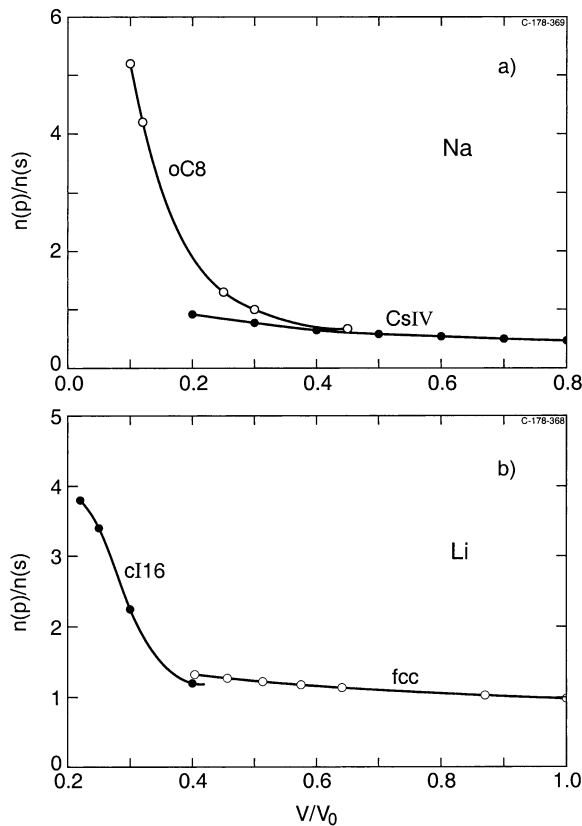


Fig. 15. Ratios between the number of p- and s valence electrons in two phases of Na (a) and two Li-phases (b). (Angular momentum projections are made onto muffin-tin spheres).

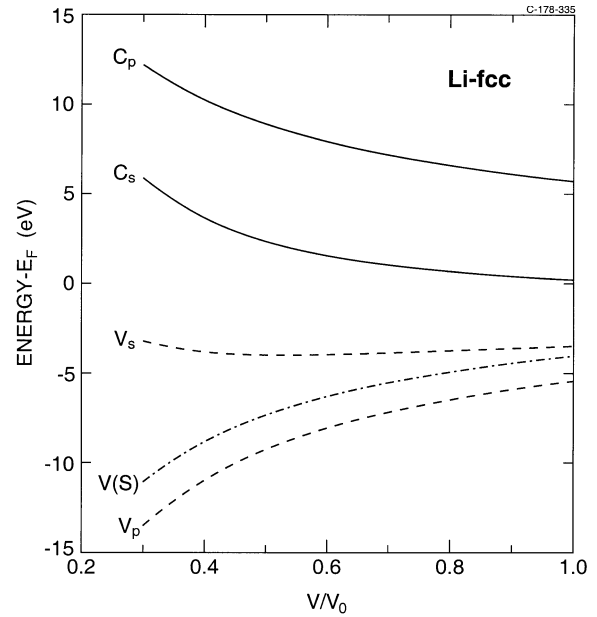


Fig. 16. Potential parameters,  $C_{s,p}$  and  $V_{s,p}$ , calculated vs. volume for the valence s- and p states in fcc-lithium in an 'ASA' (Atomic Spheres Approximation, Ref. 44). The  $C$ 's give the centers of the (unhybridized) bands, and  $V_i$  is the square-well pseudopotential for  $l$ -states. For  $s$ -states this gives the band bottom. Also shown is  $V(S)$ , the potential at the Wigner-Seitz radius. All energies are given relative to the Fermi level,  $E_F$ .  $V_0$  is the bcc-equilibrium volume of Li ( $a = 3.491$  Å).

For the free Na atom this is the same as the distance from the nucleus to the outer maximum of the Na-3s wavefunction [47]. Consequently, a 3s wavefunction from a nearest neighbor atom in the compressed solid will, when expanded around the local site, yield a very large p component. Only s states have non-vanishing amplitudes on the nucleus, and therefore the crystal structure adjusts so that there are interstitial regimes where the valence charge can pile up. This means that the coordination number is reduced to a lower value than in fcc, for example. Fig. 17(a) shows this large valence charge density in the interstitial regime of Na-oC8. The picture is quite similar to that found in the Li calculations. 'Pairs' of atoms can be seen, but, as mentioned earlier, the next-nearest neighbor distances are close to the shortest interatomic distance, and it is not very meaningful to characterize this as a solid with coordination number 1. The density plot of Fig. 17(a) further shows that the structure has some similarity with  $hP4$  (graphite type) as also can be seen from part (b) of Fig. 17. The similarity is even more obvious when comparing  $hP4$  with oC8-2, the  $Cmca$  structure derived from the Si sublattice in  $MoSi_2$ .

#### 4.2. Comparison to Li

We have already at several places compared the Na

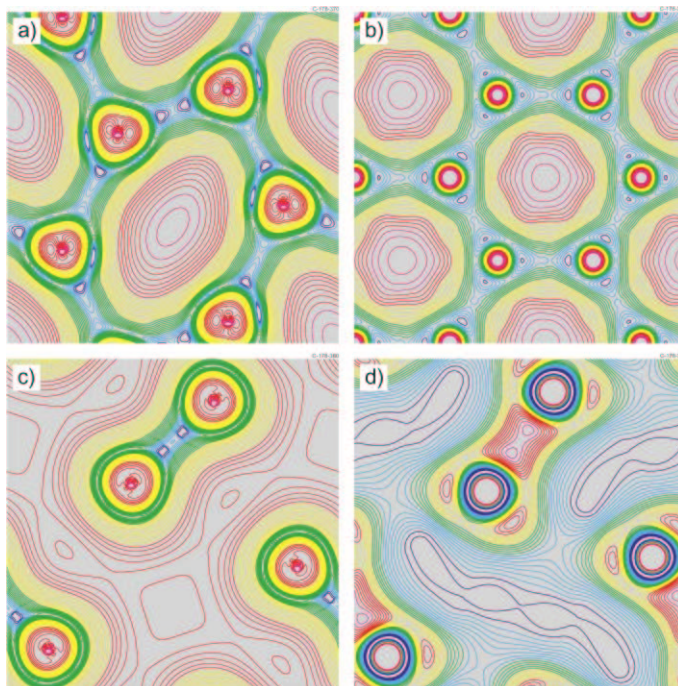


Fig. 17. Density of valence electrons, i.e. densities of core states as well as semi-core states (LO orbitals) are omitted. (a): Na-*oC8*  $V/V_0 = 0.15$ , and (b): Li-*hP4* (graphite structure), (c): Na-*BC8* at  $V/V_0 = 0.25$ , and (d): Si-*BC8*. The lowest densities are shown in blue, whereas the red (magenta) correspond to high (highest) densities.

results to experimental and theoretical results presented earlier for lithium [8,11]. Nevertheless, it is worthwhile to compare them with a larger set of data than the one which was included in our calculations in Ref. 8. Fig. 18 summarizes enthalpy calculations for 14 out of 16 examined structures. Those not included are *oC16* ('SiVI') and *R8*. The former has energies which are well above the reference in Fig. 18, and Li-*R8* was found to converge to Li-bcc at low pressures and to Li-*BC8* at high pressures. Among the interesting new results we mention those of Li-*hP4* (graphite type) and Li-*CsIV*. Li-*hP4* becomes a competitor to Li-*oC8* at very high pressures, and the calculations show that it has the lowest enthalpy above  $\approx 300$  GPa. The *CsIV* structure is even more interesting since its energy becomes very close to that of Li-*cI16* in a pressure range which may be accessed experimentally. The upper pressure attained in the measurements of Hanfland and Syassen [8] is around 55 GPa, and the present calculations suggest that there could be a pressure window starting a bit higher where Li-*CsIV* might be found. The smallest energy difference between Li-*CsIV* and *cI16* in the calculation is 1–2 meV/atom (Fig. 18), i.e. below our error bars.

Let us consider again Fig. 1 which we used as an illustration of a 'paired' high-pressure structure of an alkali metal. The valence electrons in sodium also distribute themselves in such a way, as can be seen from Fig. 17(c). The shapes of the contours between the atoms in the 'pair' resemble those

of covalent bonds. But the nature of the bonding is far from being a conventional diatomic molecular bonding. The blue contours indicate minimal densities. The valence electrons are in the interstitial regimes, and the bonding may be considered as a multicenter bonding. The bonding in the high-pressure phases of Li and Na, for example in the *oC8*, is thus quite different from that in the SiVI phase (*oC16*, also *Cmca*), see for example Fig. 6 in Ref. 48. In view of this, it is surprising how similar some of the high-pressure phases of the alkali metals are in structure to some of those found in Si and Ge. The *BC8* structure as found for Si is very similar to Li-*BC8* ( $x$  is slightly different), but the bonding is quite different. Fig. 17(d) shows our calculated density in Si-*BC8*. This may crudely be described as an 'inverse' of the Li- and Na plots.

## 5. Conclusions

The present calculations suggest that sodium and lithium both may assume several, rather complex structures under pressure. Examination of the band structures and orbital-projected density-of-states (DOS) functions show that the number of p-states is found to increase at the expense of s states under compression. The reason is that the interatomic distances become small compared to the range of the wave-functions, and the high-pressure phases become rather open.

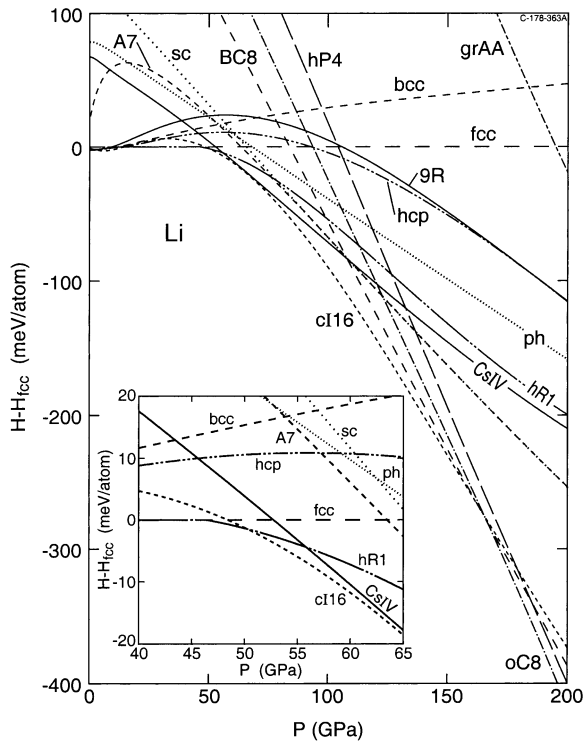


Fig. 18. Enthalpies for various Li phases vs. pressure relative to Li-fcc. (Note that the bcc was used as a reference in the case of Na). An extension of the figure would have shown the crossing near 300 GPa of the *oC8* and *hP4* enthalpy curves. The structure 'grAA' is an ...AAAAA... stacking of hexagonal layers. The inserted figure is a 'blow-up'.

Therefore, the structures found theoretically to be good candidates under very high pressures are characterized by having coordination numbers which are lower than those of the intermediate-pressure phases, bcc and fcc. In that context it is interesting to note that recent calculations by Bergara et al. [49] predict that a monolayer of lithium also would tend to form a paired structure at high densities.

The structural energy differences calculated here do not include thermal effects, i.e. vibrational contributions to energy and entropy [19,20] are neglected. This adds to the error bars of some of the tiny free energy differences. Within such limitations, the calculations for Na cannot clearly distinguish between the fcc, bcc and the *R9* structures at zero pressure. At slightly elevated pressures, though, bcc is favored, and a bcc  $\rightarrow$  fcc transition is predicted near 75 GPa. The error bar is large, probably  $\pm 20$  GPa. Na-fcc undergoes a rhombohedral deformation, and close to 130 GPa several new structures become energetically possible. Among these the *cI16* is an interesting candidate, because this structure was experimentally observed [8] for Li under pressure. Recently [29] it was also seen in Na, with an onset near 100 GPa. The present calculations suggest a stability range of Na-*cI16* to be from 130 to 170 GPa, above

which the tetragonal *CsIV* structure clearly has a lower enthalpy. Above  $P \approx 220$  GPa, we find that the Na-*oC8*, *Cmca*, may be stable up to very high pressures. The structure of Na-*oC8* is similar to the Li-*oC8* phase, but the structural parameters,  $y$ ,  $z$ ,  $bla$ , and  $cla$  vary somewhat differently with volume.

Highly compressed Na contains even more 3p- than 3s electrons and in the *oC8* the hybridization is so strong that the hybridization gap makes the DOS vanish at the Fermi level for small volumes. (In that context, see also the discussion by Neaton and Ashcroft [11] of the Peierls distortion in Li). The metal-insulator transition occurs in Na only at extreme compression. At 87% compression the *Cmca* phase is still metallic, but reduction of the volume to  $0.10 \times V_0$  produces a non-zero gap in the band structure according to the calculations. The corresponding pressure is  $\approx 950$  GPa, roughly three times the pressure at the center of the earth. For comparison, bcc-Na would need  $\approx 1500$  GPa to be compressed to  $V/V_0 = 0.10$ .

The calculations for Li, on the other hand, did not show insulating behavior in any of the phases with lowest enthalpy for  $P$  up to 4 GPa. The Li-*hP4* structure appears to be a zero-gap semiconductor at  $V/V_0 = 0.25$ , where it is not the structure with the lowest energy, though. Above 300 GPa, where its enthalpy is lower than that of Li-*oC8*, the band overlap increases, and Li becomes a 'good' metal.

As emphasized in Section 1, a theoretical study as described here is based on a comparison of a finite set of structures. Therefore, one can never be sure always to find the most stable structure, and although ab initio force calculations are used to optimize atomic coordinates, axial ratios etc. the space groups to be considered must be selected. Also, in particular for complex structures the total-energy surface may have several local minima. A systematic search for the global minimum requires methods which can pass over energy barriers. A combination of simulated annealing and 'genetic algorithms' has proven [50]<sup>2</sup> to be successful in ab initio optimization of small atomic clusters, but an implementation for crystalline solids is not straight forward. Zunger et al. [51] have used an iterative procedure where full phonon calculations are performed for several volumes of a starting structure and where symmetry analyses of soft modes are applied to identify the structure of a possible transformed phase. The method which uses group/subgroup relations where the subgroup is an 'isotropy subgroup' [52,53] applies to second order phase transitions, i.e. continuous structural deformations, and it may then be useful in prediction of deformation paths in pressure-induced transformations. Due to the complexity of some of the

<sup>2</sup> Small clusters are structurally optimized, without any symmetry constraints, by means of force calculations (real-space LMTO as developed by M. Methfessel (private communication)) combined with genetic algorithm 'mating' within an ensemble of 'parent clusters' determined by a Boltzman distribution over energy at a temperature which is gradually decreased (simulated annealing).

high-pressure phases (even) of the ‘simple metals’ reliable phonon calculations, for example from linear-response theory as applied by Savrasov [54], require large computing resources, especially because the calculations must be performed for several volumes and structures. Therefore, our theoretical search for additional ‘candidates’ for high-pressure phases of Li and Na in the nearest future will follow the lines described in this article, and a close collaboration with experimentalists is extremely important. The reactivity of compressed Li with the diamonds in a pressure cell [8], and the need to go beyond 1 Mbar in the case of Na, make such experiments very challenging.

### Acknowledgements

The authors are grateful to K. Syassen and M. Hanfland and for many very useful discussions and suggestions, as well as for the permission to cite their experimental work [29] prior to publication. During the preparation of the present article we were informed that a theoretical work on Na under pressure was submitted for publication by J.B. Neaton and N.W. Ashcroft. We thank these authors for sending us a preprint before publication. This paper has now appeared in print [17].

### References

- [1] R.M. Martin, *Nature* 400 (1999) 117.
- [2] H.T. Hall, L. Merrill, J.D. Barnett, *Science* 146 (1964) 1297.
- [3] K. Takemura, S. Minomura, O. Shimomura, *Phys. Rev. Lett.* 49 (1982) 1772.
- [4] U. Schwarz, K. Takemura, M. Hanfland, K. Syassen, *Phys. Rev. Lett.* 81 (1998) 2711.
- [5] M. Hanfland, U. Schwarz, K. Syassen, K. Takemura, *Phys. Rev. Lett.* 82 (1999) 1197.
- [6] K. Takemura, O. Shimomura, H. Fujihisa, *Phys. Rev. Lett.* 66 (1991) 2014.
- [7] K. Takemura, N.E. Christensen, D.L. Novikov, K. Syassen, U. Schwarz, M. Hanfland, *Phys. Rev. B* 61 (2000) 14399.
- [8] M. Hanfland, K. Syassen, N.E. Christensen, D.L. Novikov, *Nature* 408 (2000) 174.
- [9] M.I. Katsnelson, G.V. Sinko, N.A. Smirnov, A.V. Trefilov, K.Yu. Khromov, *Phys. Rev. B* 61 (2000) 14420.
- [10] D. Glötzel, A.K. McMahan, *Phys. Rev. B* 20 (1979) 3210.
- [11] J.B. Neaton, N.W. Ashcroft, *Nature* 400 (1999) 141.
- [12] N.E. Christensen, D.L. Novikov,  $\Psi_k$  Newsletter 42 (2000) 76. Also from: <http://psi-k.dl.ac.uk/psi-k/highlights.html> (A brief review of our lithium and sodium calculations.)
- [13] J.B. Neaton, *Bull. Am. Phys. Soc.* 45 (2000) 1001.
- [14] N.E. Christensen, D.L. Novikov, *Bull. Am. Phys. Soc.* 46 (2001) 1199.
- [15] N.E. Christensen, D.L. Novikov, *Phys. Rev. Lett.* 86 (2001) 1861.
- [16] D.L. Novikov, N.E. Christensen, *Bull. Am. Phys. Soc.* 46 (2001) 906.
- [17] J.B. Neaton, N.W. Ashcroft, *Phys. Rev. Lett.* 86 (2001) 2830.
- [18] N.E. Christensen, D.L. Novikov, M. Methfessel, *Solid State Commun.* 110 (1999) 615.
- [19] N.E. Christensen, D.J. Boers, J.L. van Velsen, D.L. Novikov, *Phys. Rev. B* 61 (2000) R3764.
- [20] N.E. Christensen, D.J. Boers, J.L. van Velsen, D.L. Novikov, *J. Phys.: Condens. Matter* 12 (2000) 3293.
- [21] U. Schwarz, K. Syassen, A. Grzechnik, M. Hanfland, *Solid State Commun.* 112 (1999) 319.
- [22] R. Ahuja, O. Eriksson, B. Johansson, *Phys. Rev. B* 60 (1999) 14475.
- [23] K. Takemura, U. Schwarz, K. Syassen, N.E. Christensen, D.L. Novikov, I. Loa, *Phys. Rev. B* 62 (2000) R10603.
- [24] K. Takemura, U. Schwarz, K. Syassen, M. Hanfland, N.E. Christensen, D.L. Novikov, I. Loa, *Phys. Status Solidi B* 223 (2001) 385.
- [25] A.W. Overhauser, *Phys. Rev. Lett.* 53 (1984) 64.
- [26] C.M. McCarthy, C.W. Tompson, S.A. Werner, *Phys. Rev. B* 22 (1980) 574.
- [27] H.G. Smith, *Phys. Rev. Lett.* 58 (1987) 1228.
- [28] W. Schwarz, O. Blaschko, *Phys. Rev. Lett.* 65 (1990) 3144.
- [29] M. Hanfland, K. Syassen, private communication, and also mentioned at the Workshop on Science at High Pressure: Latest trends from 3rd generation sources, ESRF, Grenoble, 16–17 February 2001.
- [30] R. Sternheimer, *Phys. Rev.* 78 (1950) 235.
- [31] A.K. McMahan, *Phys. Rev. B* 29 (1984) 5982.
- [32] N.E. Christensen, Z. Pawlowska, O.K. Andersen, unpublished, 1986.
- [33] J.C. Boettger, S.B. Trickey, *Phys. Rev. B* 32 (1985) 3391.
- [34] W.G. Zittel, J. Meyer-ter-Vehn, J.C. Boettger, S.B. Trickey, *J. Phys. F: Met. Phys.* 15 (1985) L247.
- [35] K.M. Lang, A. Mizel, J. Mortara, E. Hudson, J. Hone, M.L. Cohen, A. Zettl, J.C. Davis, *J. Low Temp. Phys.* 114 (1999) 445.
- [36] K.-M. Ho, C.L. Fu, B.N. Harmon, *Phys. Rev. B* 29 (1984) 1575.
- [37] H.G. von Schnering, private communication.
- [38] A.F. Wells, *Structural Inorganic Chemistry*, Oxford University Press, Oxford, UK, 1982.
- [39] J.S. Kasper, S.M. Richards, *Acta Crystallogr.* 17 (1964) 752.
- [40] R.O. Piltz, J.R. Maclean, S.J. Clark, G.J. Ackland, P.D. Hatton, J. Crain, *Phys. Rev. B* 52 (1995) 4072.
- [41] R.J. Nelmes, M.I. McMahon, N.G. Wright, D.R. Allan, J.S. Loveday, *Phys. Rev. B* 48 (1993) 9883.
- [42] R.J. Nelmes, M.I. McMahon, in: T. Suski, W. Paul (Eds.), *High Pressure in Semiconductor Physics, Semiconductors and Semimetals* (edited by R.K. Willardson and E.R. Weber), Vol. 54, Academic Press, New York, 1998, p. 145.
- [43] J.P. Perdew, K. Burke, M. Ernzerhof, *Phys. Rev. Lett.* 77 (1996) 3865.
- [44] O.K. Andersen, *Phys. Rev. B* 12 (1975) 3060.
- [45] M. Methfessel, *Phys. Rev. B* 38 (1988) 1537.
- [46] D.J. Singh, *Planewaves, Pseudopotentials and the LAPW Method*, Kluwer Academic Publishers, Boston, 1994.
- [47] F. Herman, S. Skillman, *Atomic Structure Calculations*, PrenticeHall Inc, Englewood Cliffs, NJ, 1963.
- [48] N.E. Christensen, D.L. Novikov, *Int. J. Quantum Chem.* 77 (2000) 880.
- [49] A. Bergara, J.B. Neaton, N.W. Ashcroft, *Phys. Rev. B* 62 (2001) 8494.
- [50] N.E. Christensen, unpublished work, 1998.

- [51] A. Zunger, K. Kim, V. Ozolins, *Phys. Status Solidi B* 233 (2001) 369.
- [52] A. Saxena, G.R. Barsch, D.M. Hatch, *Phase Transitions* 46 (1994) 89.
- [53] H.T. Stokes, D.M. Hatch, *Isotropy Subgroups of the 230 Crystallographic Space Groups*, World Scientific, Singapore, 1988 pp. I-347.
- [54] S.Y. Savrasov, *Phys. Rev. B* 54 (1996) 16470.